# Effect of Flow Rate on Characterizations of $TiO_2$ Nano fibers using Electro spinning Method

**The 5th International Scientific Conference for Nanotechnology and Advanced Materials and Their Applications ICNAMA 2015 (3-4Nov.2015)**

**Muhsin A. Kudhier**
Education College, University of Al-Mustansiriyah, Baghdad.
Email:muhsinattia@yahoo.com
**Dr. Raad S. Sabry**
Sciences College, University of Al-Mustansiriyah, Baghdad.
**Dr.Yousif K. Al-Haidarie**
Sciences College, University of Al-Mustansiriyah, Baghdad.

## ABSTRACT

$TiO_2$ nanofibers with anatase structure were synthesized by an electrospinning method. X-ray diffraction measurements showed that $TiO_2$ nanofibers were polycrystalline with anatase phase. The effects of flow rate parameter on $TiO_2$ nanofibers were examined using atomic force microscopy, field emission scanning electron microscopy. The energy gap was estimated and optical behavior was studied using UV-Vis spectroscopy, and Photoluminescence spectroscopy. It was noted that the average diameter of these nanofibers increases from (82-320) nm with increasing the flow rate from (1- 10 ml/h) respectively. The length of the nanofibers reached to several microns.

**Keywords:** $TiO_2$, nanofibers, Electrospinning, flow rate.

## تأثير معدل الانسياب على خصائص الياف اوكسيد التيتانيوم النانوية باستخدام تقنية الغزل الكهربائي

**الخـــلاصـــــــة**

تم تحضيرالياف نانوية من اوكسيد التيتانيوم بتركيب اناتيس باستخدام تقنية الغزل الكهربائي.التركيب المورفولجي والتركيب النانوي لالياف اوكسيد التيتانيوم تم فحصها من خلال حيود الاشعة السينية ،المجهر الذري الماسح ، والمجهر الالكتروني الماسح .تم حساب فجوة الطاقة وكذلك السلوك البصري باستخدام مطياف الاشعة فوق البنفسجية – المرئية، ومطياف التالقية الضيائية .لقد تم دراسة تاثير عامل معدل الانسياب في تقنية الغزل الكهربائي ، حيث وجد زيادة قطر الليف النانوي من ( 95 - 144 ) نانومتر بزيادة معدل الانسياب من (1- 10 ) مل/ ساعة على التوالي.طول الليف النانوي يصل لعدة مايكرونات.

## INTRODUCTION

Titanium dioxide or titania ($TiO_2$) is one of the most common materials for a variety of applications such as catalytic devices, sensors, solar cells, and other optoelectronic devices [1,2]. Titania is a wide bandgap semiconductor with many interesting properties, such as transparency to visible light, high refractive index and low absorption coefficient. Other than these properties, it has been known to be an excellent catalyst in the field of photocatalytic decomposition of organic materials. Therefore, titania has been employed for organic pollutant treatment in the environmental applications [3]. Titania is known to have three natural polymorphs, i.e. rutile, anatase, and brookite. One-dimensional nanostructures such as nanorods, nanowires, nanofibers and nanotubes of various oxide materials have been the subject



https://doi.org/10.30684/etj.2015.117364
2412-0758/University of Technology-Iraq, Baghdad, Iraq

of considerable attention in recent years. The enormous amount of attention results from fundamental scientific interest in these materials as well as from their potential applications in various types of functional devices [4-6]. Numerous methods have been developed for the fabrication of one-dimensional $TiO_2$ nanostructures, such as self-assembling, template growth, strong alkali treatment, thermal evaporation and electrospinning.

Compared to other techniques, electrospinning offers advantages of simplicity, process controllability, low production cost, and scalability for producing industrial quantities [7]. Moreover, electrospinning technique has attracted extensive interest in various areas, including photocatalysis, gas sensor, lithium-ion batteries, dye sensitized solar cells, and transparent conductive films [8-12]. Electrospinning technique has been widely used to fabricate different nanostructures (nanobelts, nanotubes and nanofibers) [13-15].

Electrospinning has been widely used to synthesize nanofibers of oxide materials [16,17]. In the typical process of electrospinning, an electrical potential is applied between a syringe needle and a grounded target. When the electrostatic force exceeds the surface tension of the droplet formed at the tip of a syringe needle, charged fluid jet is ejected which is subsequently stretched to form a continuous ultrathin fiber and finally nanofibers are deposited on a target plate [18]. During its flight to a collective target, the ejected, charged jet dries out, leaving ultra thin fibers on the target. The non-woven mat has a high surface area with relatively small pore size [1, 2, 19].

The following parameters and processing variables affect the electrospinning process: (i) system parameters such as molecular weight, molecular weight distribution and architecture (branched, linear, etc.) of the polymer, and polymer solution properties (viscosity, conductivity, dielectric constant, and surface tension, charge carried by the spinning jet) and (ii) process parameters such as electric potential, flow rate and concentration, distance between the capillary and collection screen.(iii) ambient parameters such as temperature, humidity and air velocity in the chamber . For instance, the polymer solution must have a concentration high enough to cause polymer entanglements yet not so high that the viscosity prevents polymer motion induced by the electric field. The solution must also have a surface tension low enough, a charge density high enough, and a viscosity high enough to prevent the jet from collapsing into droplets before the solvent has evaporated [20].

The aims of the present work are to prepare $TiO_2$ nanofibers by electrospinning technique using polyvinylpyrrolidone (PVP) and Ti tetraisopropoxide as precursors, and the effect of the flow rate as one of important processing parameters was then investigated on the crystal structure, morphology, and microscopy of electrospun $TiO_2$ nanofibers. $TiO_2$ nanofibers were characterized by XRD, AFM, SEM, UV-Vis, and PL spectroscopy.

## Experimental

The chemicals used in this study were high purity titanium tetraisopropoxide (TIP) (Ti [OCH $(CH_3)_2]_4$, 97% Sigma Aldrich,), polyvinylpyrrolidone (PVP, Sigma Aldrich Mw = 1,300,000), acetic acid ($CH_3COOH$, 99.7% Scharlau, Spain), ethanol (99%Scharlau, Spain).

In a typical procedure, 1 g of titanium tetraisopropoxide (TIP) was mixed with 2 ml of acetic acid and 2 ml of ethanol. The solution was rested for 10 min before being added into 5 ml of PVP solution in ethanol. The concentration of the PVP solution was kept 7 wt% and the resulting mixture was constantly stirred for 10 min. The

spinning solution was immediately loaded into a plastic syringe with 21-gauge stainless steel needle was used as the nozzle. The emitting electrode from a Gamma High Voltage Research ES30P power supply capable of generating DC voltages up to 25 kV was attached to the needle. The grounding electrode from the same power supply was attached to a plate of aluminium with clean glass substrates fixed on it which was used as the collector plate and was placed 20 cm in front of the tip of the needle. When an applied voltage of 21 kV is subjected across the needle and the collective plate, a fluid jet was ejected from the nozzle. The feed rate of the precursor solution was (1, 5, and 10 ml/h) which can be controlled using a syringe pump (KDS 200). As the jet accelerated towards the collector, the solvent evaporated, leaving only ultra-thin fibers on the collector as shown in figure (1). The obtained fibers were left exposed to moisture for approximately 10 h to allow complete hydrolysis of TIP and consequently subjected to calcination at a high temperature of 500 $^{o}$C for 3 h with a heating rate of 5$^{o}$C/min to remove residual PVP.

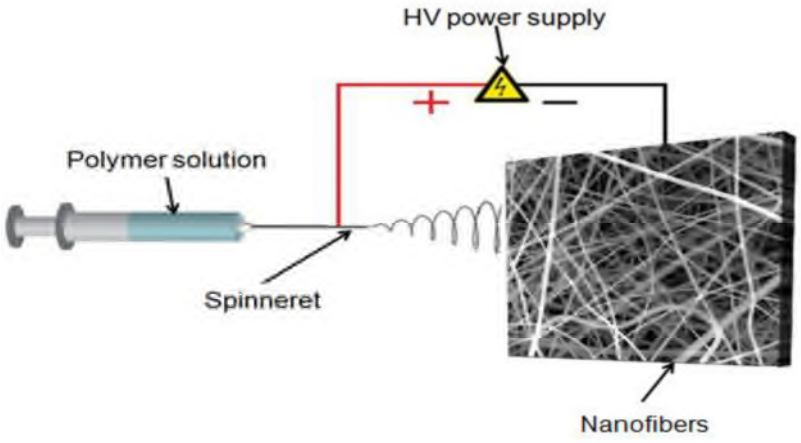


**Figure (1) Schematic view of electrospinning technique.**

The x-ray diffraction (XRD) measurements, which were used to characterize the crystalline phase of the $TiO_2$fiber, were carried out on an x-ray diffractometer (type miniflex II Rigaku, Japan) using (CuKα) radiation. Atomic force microscopy (AFM) micrographs were taken with a Digital Instruments, Inc. Nanoscope III and Dimension 3100). The samples were observed under a (Hitachi S-4160 Japan) field emission scanning electron microscope (FESEM) after being gold-coated. The optical absorption spectra of the $TiO_2$ film were recorded using (Optima Sp-3000 plus UV-Vis-NIR, Split- beam Optics, Dual detectors) spectrophotometer equipped with a xenon lamp and a wavelength range of (300- 900 nm).The photoluminescence (PL) spectra were recorded at room temperature (25 $^{o}$C) using the (Perkin Elmer Spectrophotometer Luminescence LS 55) by exciting the samples at 260 nm.

**Results and discussion**

Figure (2) shows the XRD patterns of the as-prepared samples calcined at 500 $^{0}$C for 3 hours in air atmosphere. The peaks shown in the XRD patterns correspond to the (101), (004), (112), (200), (105), (211), and (204) planes of $TiO_2$ tetragonal anatase phase. These patterns can be well indexed to tetragonal anatase (JCPDS no. 21- 1272). No peaks of brookite or rutile phase were detected, which indicate the high

purity of the as-prepared samples. The crystallite size can be estimated using the Scherrer formula [21]:

$$D = k\lambda / \beta \cos \theta \quad \ldots(1)$$

Where:

D is the crystallite size in nanometers, k a constant (=0.9 assuming that the particles are spherical), $\lambda$ is the wavelength of the X – ray radiation (CuK$\alpha$ =0.1541 nm), $\beta$ is the FWHM of the strongest peak, and $\Theta$ is the diffraction angle. The crystallite sizes of the powders were calculated on the diffraction peaks of anatase (101) crystalline plane. According to these calculations, the crystallite sizes of the fibers were (23.52, 24.15, 26.00 nm), for the fibers prepared in (1, 5, 10 ml/h) respectively. These results revealed that the resultant fibers obtained in different flow rates were all in the $TiO_2$ anatase phase, and with an increase of the flow rates, crystallites size of the samples was getting larger. Also, it can be found that films prepared in high flow rate show relative sharp peaks indicating the coalescence of crystalline anatase phase $TiO_2$.

The surface morphology and roughness have been indicated in figure (3) using AFM images, the roughness average is (10.30, 5.15, 3.97 nm) for the fibers prepared in (1, 5, 10 ml/h) respectively. The roughness average increased with the flow rate decreased, and this has great advantages in many applications of $TiO_2$ nanofibers such as sensing and photocatalyst applications.

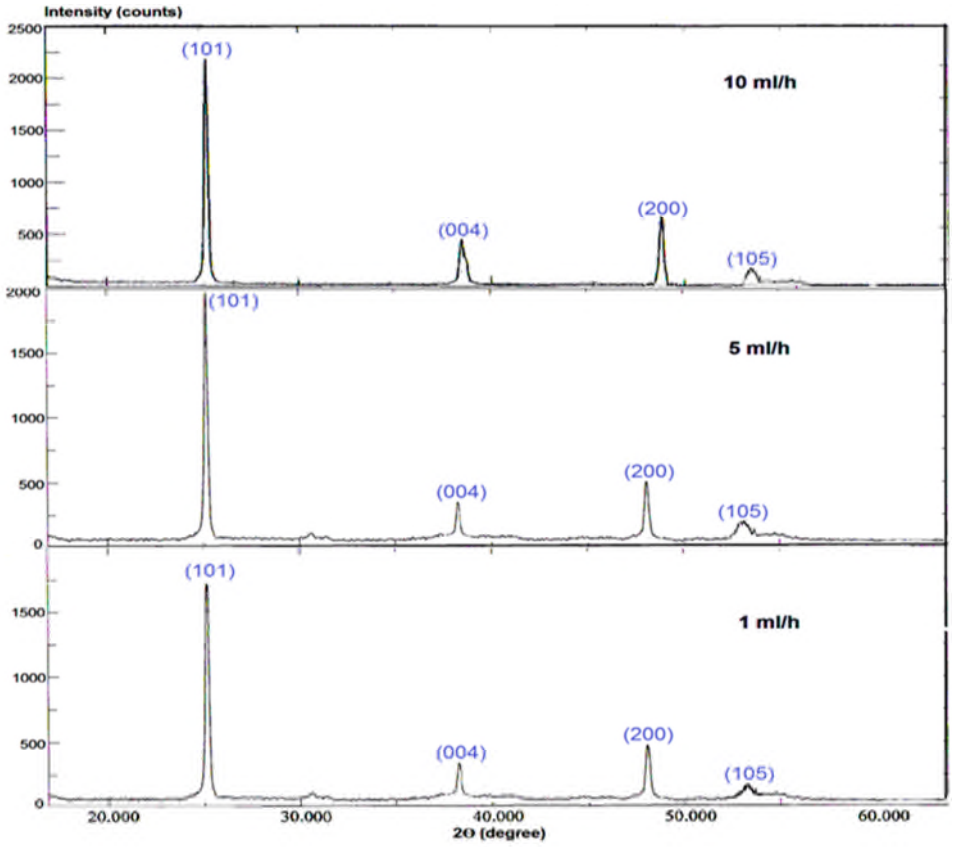


**Figure (2) XRD spectra of $TiO_2$ fibers prepared in different flow rates**

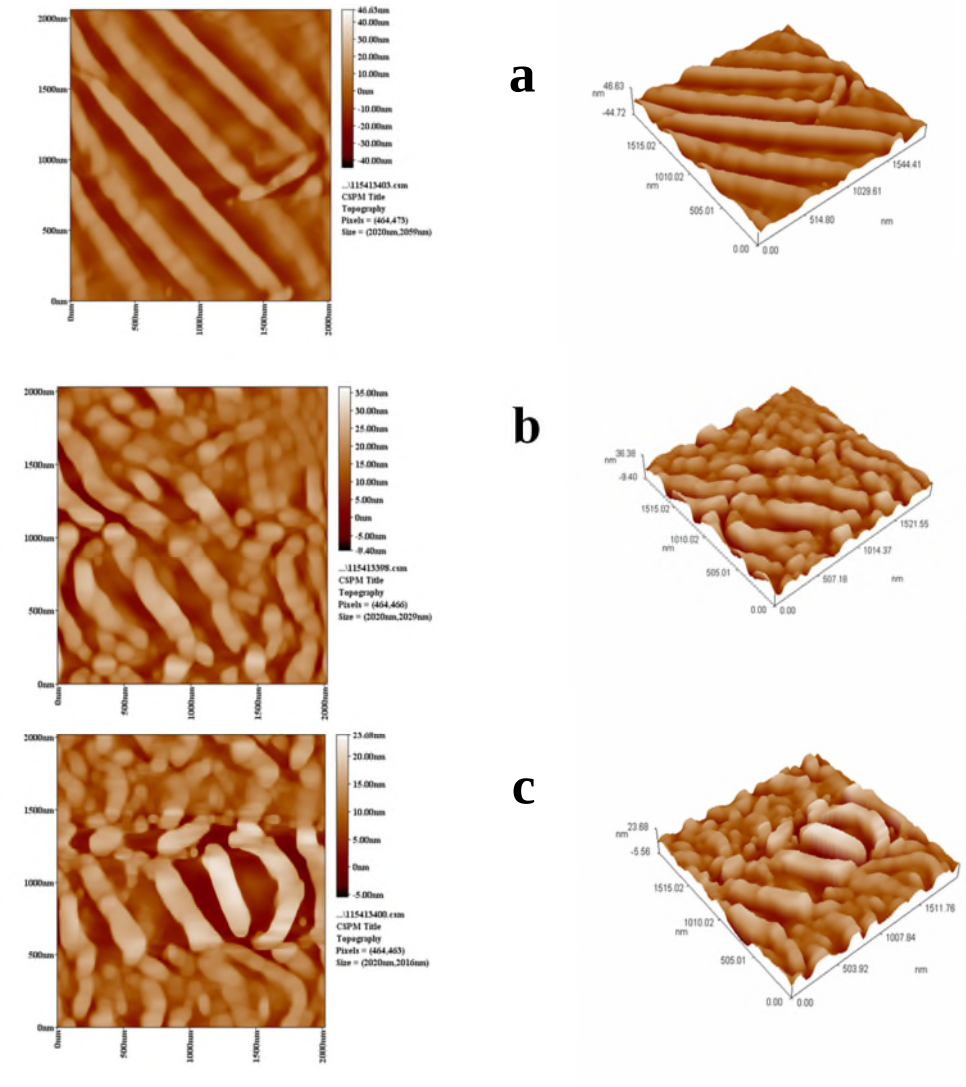


**Figure (3) : AFM micrographs of $TiO_2$ fibers prepared in different flow rates (a) 1 ml/h (b) 5 ml/h (c) 10 ml/h.**

Nanofibers were investigated by FESEM analyses. Figure (4) represents FESEM images of pre-calcined as-spun fibers and titania fibers after calcination at 500 $^{o}$C for 3h .The diameters of $TiO_2$ nanofibers ranging from (48-390 nm).The average diameters of pre-calcined as-spun fibers are (220, 345, 485 nm) , and in the calcined $TiO_2$ nanofibers are (82, 245, 320 nm) prepared in (1, 5, 10 ml/h) respectively. Figure (3d) illustrates homogenous distribution of $TiO_2$ nanofibers mats.

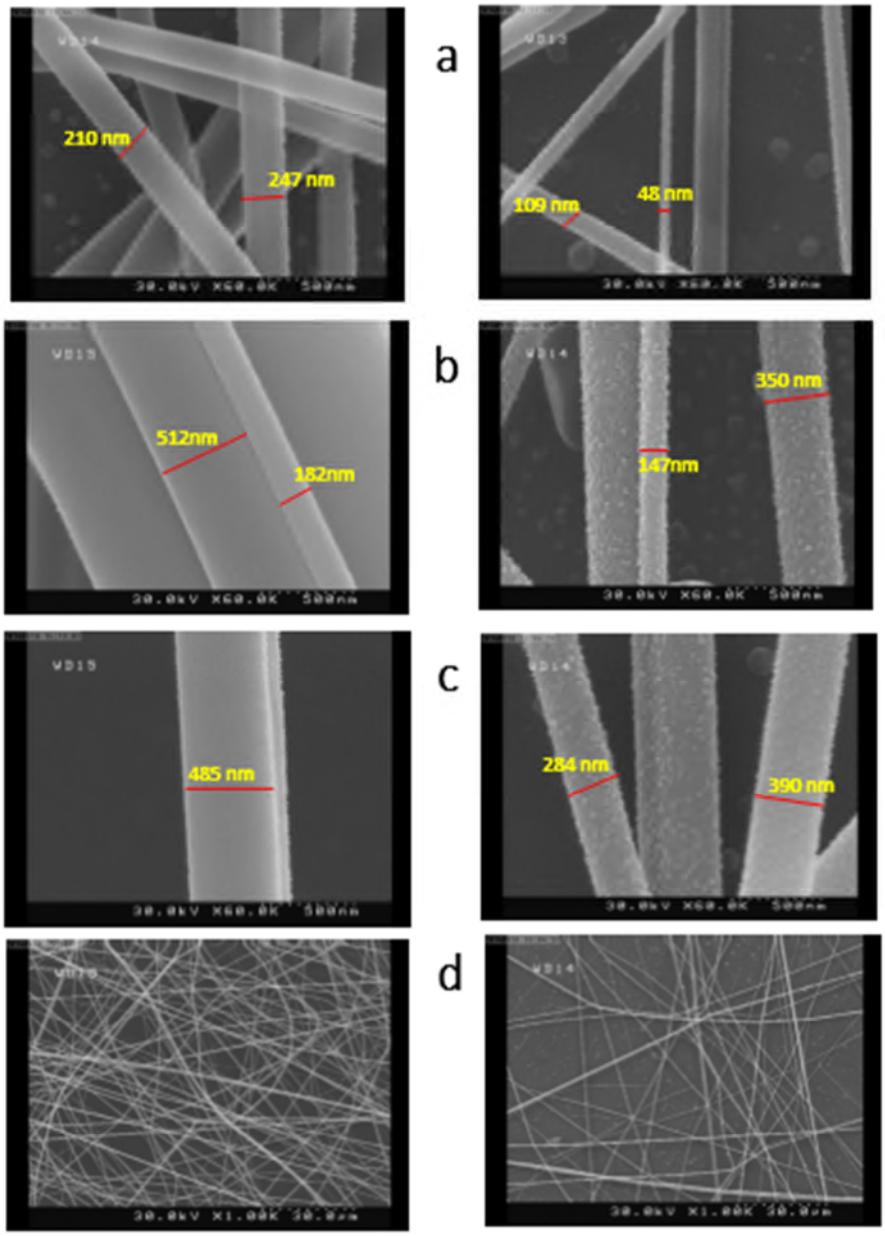


**Figure (4) FESEM images of pre-calcined as-spun fibers on left side and $TiO_2$ nanofibers on right side prepared in different flow rates (a) 1 ml/h (b) 5 ml/h (c) 10 ml/h (d) 10 ml/h in smaller magnification.**

Figure (5a) shows the variation of the transmittance with the flow rate, the transmittance decreases with increases the flow rate, while the energy gap remains unchanged and equal to (3.45 eV) as it shown in figure (5b) .This relatively large value of band gap is usually observed when we are dealing with fine particles in the nanoscale therefore this blue shift of the band gap was taken place because of the quantum confinement effect [22, 23].

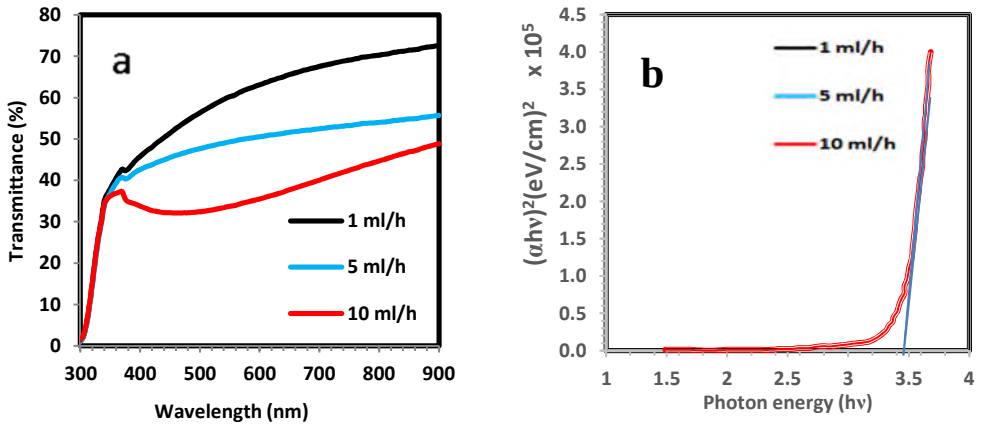


**Figure (5) (a) The transmittance vs. wavelength of $TiO_2$ nanofibers prepared in different flow rates (b) The allowed direct band gap prepared in different flow rate.**

The PL excitation spectra were evaluated in figure (6). For all samples, the PL excitation spectra have many peaks: (338,355,365, and 471 nm) which are corresponding to (3.67, 3.50, 3.40, and 2.63 eV) respectively. Hence, this band corresponds to the photo absorption near the band energy (NBE) edge of the conduction band [20]. It has been demonstrated that the occurrence of emission peak in the visible region (471 nm) is due to the presence of defect levels below the conduction band. The native defects in wide gap semiconductors are expected to introduce deep levels inside the band gap [24]. The broad luminescence spectrum in the visible region is attributed to the electronic transition mediated by the defect levels, such as oxygen vacancies in the band gap [25]. The stronger the PL intensity, the larger the content of oxygen vacancies and defects, and this occurred with increases the flow rate.

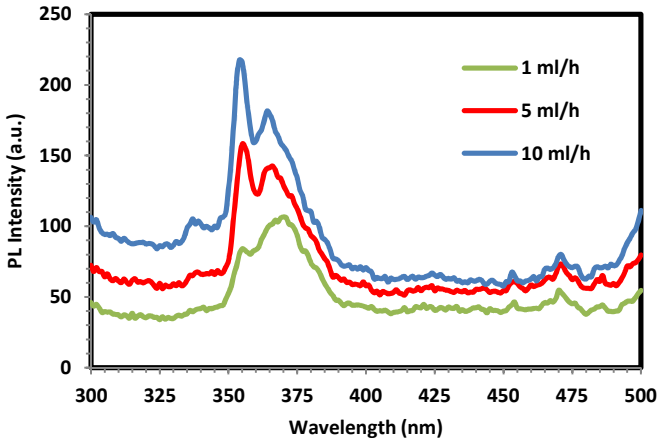


**Figure (6) PL spectra of $TiO_2$ nanofibers prepared in different flow rates.**

## CONCLUSIONS

Nanofibers of $TiO_2$ have been successfully fabricated using an electrospinning method. This method is simple and repeatable.$TiO_2$ nanofibers (diameter of ~48–390 nm) could be obtained and confirmed by XRD and the crystalline phase in the form of pure anatase structure. It was concluded that the flow rate is an important parameter in the electrospinning method, and the effect of this parameter was studied on roughness, diameters, energy gap, and emission spectrum of $TiO_2$ nanofibers.

## REFERENCES

[1] D. Li, Y. Xia, "Fabrication of titania nanofibers by electrospinning", Nano Letters 3 (2003) 555.
[2] P. Viswanathamurthi, N. Bhattarai, C.K. Kim, H.Y. Kim, D.R. Lee, "Ruthenium-doped $TiO_2$ fibers by electrospinning", Inorganic Chemistry Communications 7 (2004) 679.
[3] C.H. Kwon, H. Shin, J.H. Kim, W.S. Choi, K.H. Yoon, "Degradation of methylene blue via photocatalysis of titanium dioxide", Materials Chemistry and Physics 86 (2004) 78.
[4] G. Yu, A. Cao, and C. M. Lieber," Large-area blown bubble films of aligned nanowires and carbon nanotubes", Nature Nanotech.2 (2007) 372.
[5] B. Tian, X. Zheng, T. J. Kempa, Y. Fang, N. Yu, G. Yu, J. Huang, and C. M. Lieber," Coaxial silicon nanowires as solar cells and nanoelectronic power sources", Nature 449 (2007) 885.
[6] W. Lu and C. M. Lieber, "Nanoelectronics from the bottom up", Nature Mater. 6 (2007) 841.
[7] A. Kumar, R. Jose, K. Fujihara, J. Wang, S. Ramakrishna," Structural and Optical Properties of Electrospun $TiO_2$ Nanofibers", Chem. Mater. 19 (2007) 6536. [8] W. Zhang, R. Zhu, X. Liu, B. Liu, S. Ramakrishna," Facile construction of nanofibrous ZnO photoelectrode for dye-sensitized solar cell applications", Appl. Phys. Lett. 95 (2009) 043304.
[9] B. Ding, M. Wang, J. Yu, G. Sun, "Gas Sensors Based on Electrospun Nanofibers", Sensors. 9 (2009)1609.
[10] D. Lin, H. Wu, R. Zhang, W. Pan," Enhanced Photocatalysis of Electrospun Ag−ZnO Heterostructured Nanofibers", Chem. Mater. 21 (2009) 3479.
[11] L. Ji, Y. Yao, O. Toprakci, Z. Lin, Y. Liang, Q. Shi, A.J. Medford, C.R. Millns, X. Zhang, "Fabrication of carbon nanofiber-driven electrodes from electrospun polyacrylonitrile/polypyrrole bicomponents for high-performance rechargeable lithium-ion batteries", J. Power Sources. 195 (2010) 2050.
[12] H. Wu, L. Hu, M.W. Rowell, D. Kong, J.J. Cha, J.R. McDonough, J. Zhu, Y. Yang, M.D. McGehee, Y. Cui, "Electrospun Metal Nanofiber Webs as High-Performance Transparent Electrode", Nano Lett. 10 (2010) 4242.
[13] D. Li, Y. Xia, "Electrospun Metal Nanofiber Webs as High-Performance Transparent Electrode", Adv. Mater. 16 (2004) 1151.
[14] W. Wang, J. Zhou, S. Zhang, J. Song, H. Duan, M. Zhou,C. Gong, Z. Bao, B. Lu, X. Li, W. Lan, E. Xie, "A novel method to fabricate silica nanotubes based on phase separation effect", J. Mater.Chem. 20 (2010) 9068.
[15] Y. Su, B. Lu, Y. Xie, Z. Ma, L. Liu, H. Zhao, J. Zhang, H. Duan, H. Zhang, J. Li, Y. Xiong, E. Xie," Temperature effect on electrospinning of nanobelts: the case of hafnium oxide", Nanotechnology. 22 (2011) 285609.

[16] Z. Liu, D. D. Sun, P. Guo, and J. O. Leckie," An Efficient Bicomponent $TiO_2/SnO_2$ Nanofiber Photocatalyst Fabricated by Electrospinning with a Side-by-Side Dual Spinneret Method" , Nano Lett. 7 (2007)1081.
[17] M. M. Munir, F. Iskandar, K. M. Yun, K. Okuyama, and M. Abdullah,"Optical and electrical properties of indium tin oxide nanofibers prepared by electrospinning", Nanotechnology 19 (2008)145603.
[18] D. Li, Y. L. Wang, and Y. N. Xia, "Electrospinning Nanofibers as Uniaxially Aligned Arrays and Layer-by-Layer Stacked Films", Nano lett. 3 (2003)1167.
[19] C. Mit-uppatham, M. Nithitanakul, P. Supaphol, "Ultrafine electrospun polyamide-6 fibers: effect of solution condition on morphology and average fiber diameter", Macromolecular Chemistry and Physics 205(2004) 2327.
[20] Ioannis S. Chronakis, "Novel nanocomposites and nanoceramics based on polymer nanofibers using electrospinning process",A review, Journal of Materials Processing Technology 167 (2005) 283.
[21]A. L. Patterson, "The Scherrer Formula for X-Ray Particle Size Determination", Phys. Rev. 56 (1939) 978.
[22] Wiwat Nuansing, Siayasunee Ninmuang, Wirat Jarernboon, Santi Maensiri, Supapan Seraphin ." Structural characterization and morphology of electrospun $TiO_2$ nanofibers" Materials Science and Engineering B 131 (2006) 147.
[23] Y. Dzenis," Spinning continuous fibers for nanotechnology", Science 304 (5679) (2004) 1917.
[24] R. Sarkar, C. S. Tiwary, P. Kumbhakar, S. Basu and A. K. Mitra," Yellow orange light emission from $Mn^{+2}$ -doped ZnS nanoparticles", Physica E, vol. 40 ( 2008) 3115.
[25] R. N. Bhargava, D. Gallagher, "Optical properties of manganese-doped nanocrystals of ZnS", Physics Review Letters, vol. 72(1994) 41.